WPHCD-PR(17) 18698

A Mimo et al.

Investigation of caesium flow in negative hydrogen ion sources for ITER

Preprint of Paper to be submitted for publication in
Plasma Physics and Controlled Fusion

This work has been carried out within the framework of the EUROfusion Consortium and has received funding from the Euratom research and training programme 2014-2018 under grant agreement No 633053. The views and opinions expressed herein do not necessarily reflect those of the European Commission.

Investigation of caesium flow in negative hydrogen ion sources for ITER

A. Mimo, C. Wimmer, D. Wünderlich and U. Fantz

Max-Planck-Institut für Plasmaphysik, Boltzmannstr. 2, 85748 Garching, Germany

E-mail: alessandro.mimo@ipp.mpg.de

Abstract. The Neutral Beam Injection (NBI) systems for the fusion experiment ITER rely on the neutralization of negative H^-/D^- ion beams. Negative ions are produced in the ion sources mainly by surface conversion of H/D atoms on a converter surface: in order to reach a high conversion efficiency the work function of the converter surface is lowered by seeding Cs into the source. The maintenance of a sufficient Cs flux onto the converter surface is needed in order to counteract the degradation of the work function during the beam pulse. Numerical simulations were performed in order to study the emission profile of the different Cs seeding nozzle geometries which are used in the ITER relevant negative ion sources at the test facilities BATMAN and ELISE. These results are taken as input for the Monte Carlo transport code `CsFlow3D`, which simulates the evaporation of Cs inside the source and its redistribution during plasma phases. Simulations for the prototype source have shown that the positioning and the orientation of the Cs nozzle influence Cs redistribution during the pulse and that a repetition of consecutive pulses leads to an overall increase of Cs flux onto the converter surface. `CsFlow3D` was then applied to a specific configuration of the BATMAN test facility in order to find the best position of the Cs oven nozzle.

PACS numbers: 52.50.Dg, 52.65.Pp

Keywords: Negative ion source, caesium dynamics, caesium modelling, Neutral Beam Injection

1. Introduction

The most powerful plasma heating system in ITER is based on the Neutral Beam Injection (NBI), i.e. the injection of neutral particles which can deliver energy to the plasma by means of collisions and can also be used for current drive. Two NBI systems will provide a total power of 33 MW at an acceleration energy equal to 1 MeV for D^- ions and 870 keV for H^-[1]. These systems are based on the neutralization of a high energetic ion beam: the neutralization efficiency for positive ions at the required energy is very low and so negative ions have to be used, for which the neutralization efficiency in the case of an optimized gas neutralizer is equal to 60% at this energy [2]. The total accelerated negative ion current that has to be delivered by each source is 48 A in

hydrogen and 40 A in Deuterium, for one hour and with a ratio between co-extracted electrons and negative ions below one [1]. In order to limit the stripping process of D^- by collisions with background gas inside the accelerator, the source has to be operated at a pressure below 0.3 Pa [3]. The main production mechanism of negative ions relies on the conversion of neutral H/D on a metallic converter surface with a conversion efficiency that increases with decreasing surface work function. In order to achieve a low work function, cesium is evaporated inside the source [4, 5, 6].

The ITER NBI system will rely on RF driven negative ion sources: the RF prototype source with the size of 1/8 of the ITER source (59 cm x 30 cm) is in operation at the BATMAN test facility [7]. Beside the prototype source, a larger source, half of the ITER size (100 cm x 90 cm), is also in operation at the ELISE test facility [8].

2. Prototype source

Figure 1 shows the prototype source, where the main parts are highlighted. The plasma is generated by inductive RF coupling inside the driver and it expands in the expansion chamber, towards the plasma grid. Permanents magnets are installed in the diagnostic flange in order to reduce the electron temperature in the region where the negative ions are generated: a reduction of the electron energy is needed to limit the electron detachment process of negative ions due to collision with electrons [9]. Negative ions are then extracted and accelerated at a maximum energy of 22 keV by a three grid system: the plasma grid (PG) facing the plasma, the extraction grid and the grounded grid.

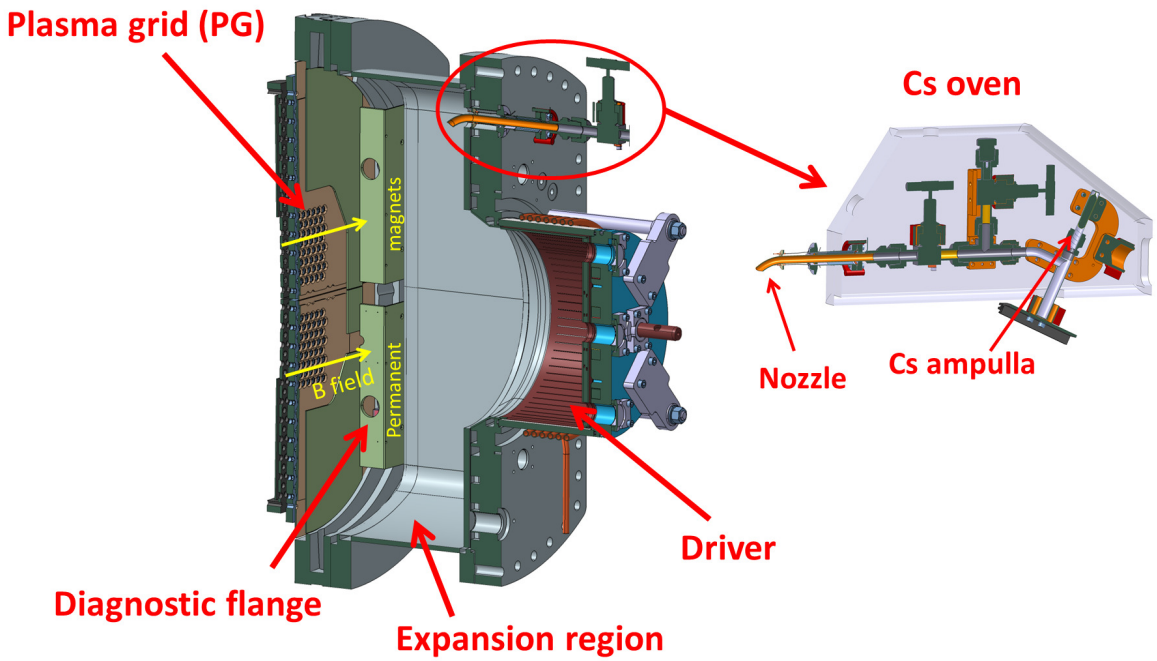

Figure 1: Prototype source at the BATMAN test facility.

The operation of the prototype source at BATMAN is pulsed, i.e. it consists of two phases: the vacuum phase with a duration of ~ 4 minutes, and a background gas pressure of $\sim 10^{-4}$ Pa; the plasma phase, when RF power up to 100 kW is applied for up to $\sim$7.5 s, with a hydrogen filling pressure in the range 0.3 Pa - 0.6 Pa. Inside the driver the plasma density is $\sim 10^{18}\,\mathrm{m}^{-3}$ and electron temperature is ~ 10 eV, while close to the plasma grid these values are reduced to $\sim 10^{17}\,\mathrm{m}^{-3}$ and ~ 1 eV respectively.

Cs seeding occurs in both vacuum and plasma phases and it is based on the evaporation of liquid Cs by means of a Cs oven like the one shown in Figure 1. A reservoirs of 1 g liquid Cs is heated up to temperatures between 100°C and 150°C in standard operation. An increase in temperature determines an increase of the Cs vapour pressure and then of the flux of Cs, which is evaporated into the source through a nozzle. A relative measurement of the evaporation rate is performed by means of a surface ionization detector (SID) located in front of the nozzle exit: the estimated value of the evaporation rate for standard operation is 10 mg/h [10]. In order to avoid sticking of Cs inside the oven conduction pipe and inside the nozzle, these parts are heated up to high temperatures, namely above 250°C. To stop Cs evaporation, the heating of the Cs reservoirs is turned off and the oven volume can be sealed by closing a valve. The standard position of the Cs nozzle used in the experimental campaigns is on the top of the back-plate and the evaporation is directed towards the plasma grid, as in figure 1.

The source performance strongly depends on the Cs conditioning of the plasma grid, which can be influenced by two effects: the plasma removal of the Cs deposited on the plasma grid and the degradation of the deposited Cs layers due to the reaction with impurities. The background gas pressure during the vacuum phase (between 10^{-5} and 10^{-4} Pa) is in fact far from the ultra high vacuum conditions and therefore the presence of impurities play a dominant role for the source performances [11] due to the creation of Cs compounds. It has been observed that without providing a sufficient flux of Cs, a degradation of the work function occurs [12], thus implying worse performances.

The achievement of good and stable performances (i.e. high extracted negative ion and low co-extracted electron currents) is therefore connected with the maintenance of a sufficient and homogeneous Cs flux onto the plasma grid. To reach this target, an improvement of the Cs management in negative ion sources is needed: in particular the Cs dynamics and the plasma assisted redistribution of Cs during the plasma phase are still not completely understood. A better Cs management in the source can also help in reducing the Cs consumption. For these reasons Cs dynamics have been investigated by means of numerical simulations with the `CsFlow3D` code, as described in the following section.

3. CsFlow3D code for simulation of Cs dynamics

The Monte Carlo transport code `CsFlow3D` was developed to simulate Cs transport and redistribution in large negative ion sources and preliminary simulations of the prototype source at the MANITU test facility were performed [13]. The main purpose of the code

is to calculate the Cs fluxes onto the plasma grid as well as the Cs coverage on the inner surface of the source.

The Cs transport is modeled differently for the vacuum phase and for the plasma phase. During the vacuum phase the collisions between the Cs particles and the background gas are neglected due to the low pressure and the Cs transport has been modeled as ballistic. The Cs evaporated from the oven can deposit onto the source walls with a sticking probability which depends on the temperature of the surface and on the presence of impurities, due to the high reactivity of Cs. Due to the lack of data in literature regarding the Cs sticking coefficients for the specific conditions of the ion sources, the values of the sticking coefficient are based on experiments performed in a smaller source operating at similar conditions of the prototype source [14]. In order to use the proper value of sticking, in the simulation the temperature of the source walls is set to 35°C and the plasma grid temperature to 150°C, which are typical values used in the experiment with the prototype source.

During the plasma pulse collisions are considered and treated via Monte Carlo methods [15]. The electron impact ionization of Cs have to be taken into account due to the low ionization energy of Cs (3.89 eV) [16]. Secondary ionization of Cs is neglected due to the higher ionization energy (23.8 eV) [17], so only singly ionized Cs ions are considered. Also collisions with the molecular hydrogen background gas and the positive hydrogen ions are taken into account: a detailed description of the collision treatment of `CsFlow3D` can be retrieved in [18]. Beside the evaporation from the oven, another source term of Cs has to be considered: the Cs deposited on the walls can be removed by plasma contact and tansported by means of collisions.

An important input parameter for the code is the Cs nozzle outflow profile, which depends on the geometry of the nozzle. In order to determine this profile numerical simulations were performed for two slightly different geometries of the nozzle used in the negative ion sources at IPP and the results are shown in section 4.

During the vacuum phase the Cs flux and therefore the coverage onto the plasma grid is determined by the direct evaporation from the oven, so spatial inhomogeneity can be expected. A different situation occurs during the plasma phase, since the Cs transport relies instead on plasma redistribution. The Cs dynamics can therefore be affected by the accumulation pattern of Cs on the source walls, determined by the Cs nozzle configuration. In order to investigate this effect, `CsFlow3D` was applied to the prototype source and simulations were performed for different nozzle positions and orientations. The purpose was to investigate the effect of these parameters in order to identify the condition in which the best Cs redistribution occurs (i.e. a sufficient and homogeneous flux) and to find a strategy to optimize the configuration of Cs oven.

4. Cs nozzle outflow profile

The emission pattern of the Cs oven nozzles used in the negative ion sources at the BATMAN and ELISE test facilities has been investigated by means of Direct Simulation

Monte Carlo (DSMC) [19], a numerical method which allows modelling the flow of rarefied gas. The code used for the simulation can be retrieved at [20]. Two different nozzle types with an inner diameter of 8 mm were considered: in case A the nozzle has a 45° angle cut; in case B the nozzle is instead bent of 45° and straightly cut.

Figure 2a shows the contour plot of the Cs fluxes calculated for the two different nozzle types. It is evident that the maximum of the flux appears at different angles in the two cases: in the case A, the maximum flux occurs at 25° with respect to the horizontal direction and in the case B it appears at 45°. This is clear also by observing the polar plot of the normalized flux in figure 2b: there are no relevant differences in the emission profiles between the two nozzle types, except for the angle shift. The simulated outflow profile can be fitted by a squared cosine function.

The results of this simulation are useful to model the angular distribution of Cs particles evaporated from the nozzle. The evaporation rate depends on the temperature of the Cs liquid reservoirs and on the Cs transport along all the complete geometry of the oven, which is not taken into account by the DSMC simulations. For this reason the evaporation rate in `CsFlow3D` was set to the experimental value of 10 mg/h [10].

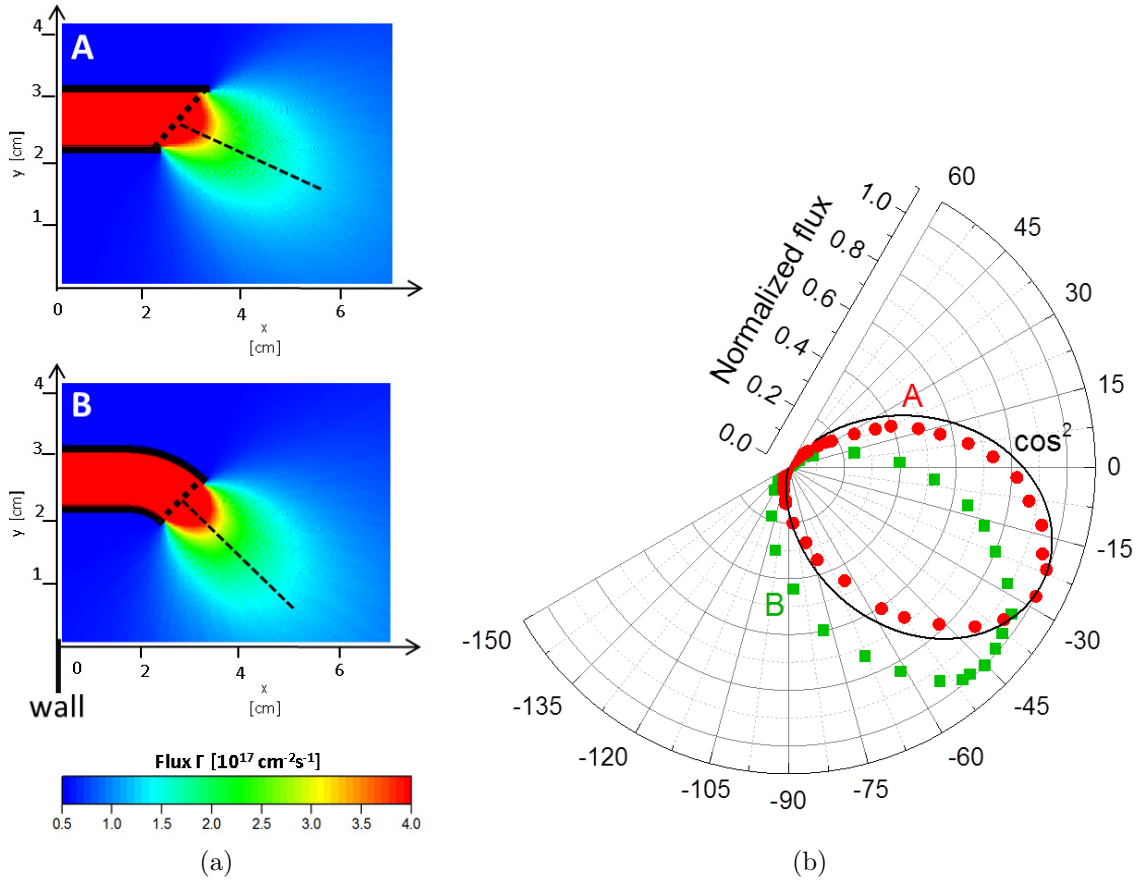

(a) (b)

Figure 2: (a) Contour plot of the Cs flux evaporated by the two different nozzle geometries; (b) Polar plot of the Cs emission profile of the nozzles and the $\cos^2$ fitting function for case A.

5. Effect of nozzle orientation and position

As a first step a clean source was considered, i.e. with no Cs deposited on the walls: a simulation of one vacuum phase of 240 s followed by a plasma pulse of 8 s was performed (these are typical values adopted during the experiments), with the nozzle in the standard position, i.e. in the back-plate and a downwards bending angle of 50°. The nozzle length inside the source is 2.5 cm, as in figure 2a. This simulation was performed once by considering a continuous Cs evaporation, during both vacuum and plasma phase, and a second time by stopping Cs evaporation during the plasma phase. By comparing the two cases it is possible to determine if the leading source term of Cs during the plasma phase is the evaporation from the oven or the Cs release due to plasma erosion.

Figure 3 shows the evolution in time of the total Cs flux (i.e. the sum of both neutral Cs particles and positive Cs ions) averaged onto the PG area in the two cases, with and without Cs evaporation in plasma. It is evident in both cases that the Cs flux is higher during the plasma phase w.r.t. the vacuum phase, due to plasma erosion. The difference of the flux in the two cases, with and without Cs evaporation in plasma is below 10%, thus proving that the erosion of Cs is the leading source term in plasma.

All the plasma parameters during the pulse are constant, so the time evolution that can be observed in the simulated fluxes is only due to the dynamics of Cs. The built up of Cs reservoirs can therefore affect the amount of Cs released during the plasma phase and in particular a different location of these reservoirs in the source walls may lead to different Cs fluxes onto the PG. Since the location of these reservoirs depends on the orientation of the nozzle, calculation were performed with `CsFlow3D` for different nozzle bending angles. In the first simulation campaign the Cs oven nozzle was positioned in

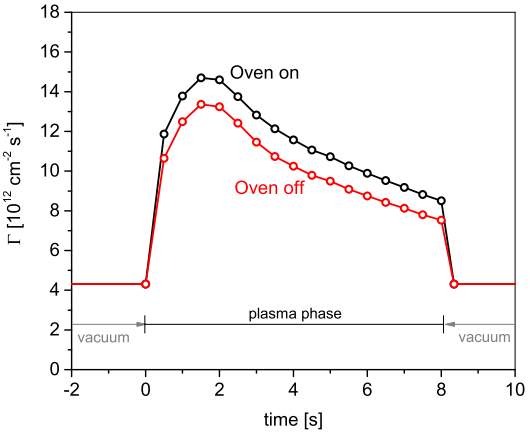

Figure 3: Evolution in time during the plasma pulse of the total Cs flux Γ (i.e. neutral Cs and Cs^+) averaged over the PG area: in red without Cs evaporation in plasma, in black with evaporation.

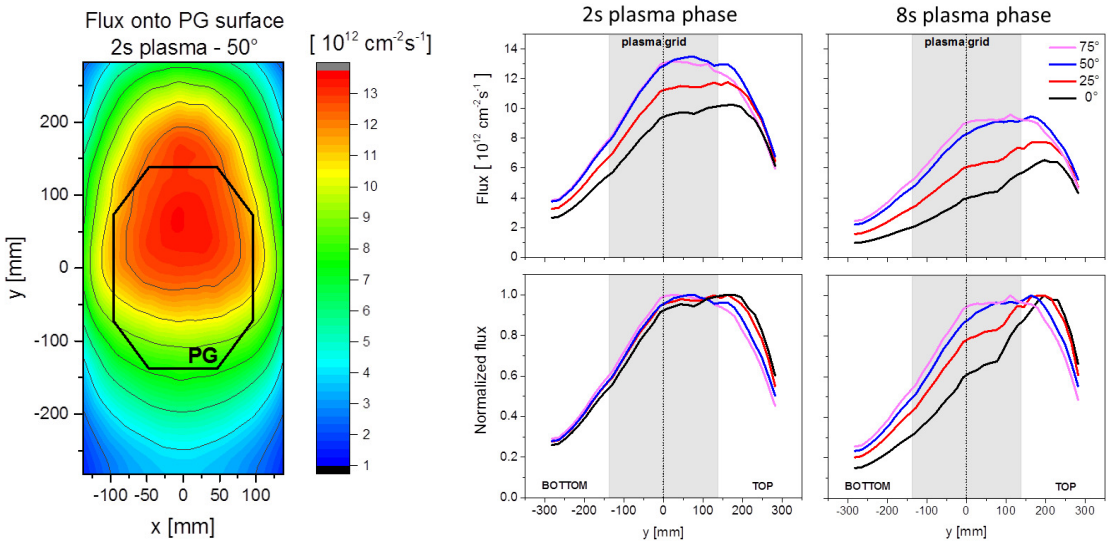

(a) (b)

Figure 4: (a) Total Cs flux (i.e. neutral Cs and C^+) onto the plasma grid for the 50° case after 2 s of plasma; (b) Cut plot at x = 0 of Cs total flux at the beginning of the plasma pulse (t = 2 s) and at the end of the pulse (at t = 8 s). Top: absolute flux, bottom: normalized values.

the standard location, i.e. in the uppermost part of the prototype source back-plate, at four different inclination angles (0°, 25°, 50°, 75°).

Figure 4a shows a contour plot of the total Cs flux (i.e. neutral and ions) onto the plasma grid wall at $t = 2$ s for the orientation at 50°. The ionization degree of Cs that impinge the PG depends on the position, in average the Cs ions represent $\sim 70\%$ of the total Cs. In order to investigate the time evolution of the flux profile for the different angles, the cut plots at $x = 0$ at time $t = 2$ s and at the end of the pulse ($t = 8$ s) are shown in figure 4b: the two plots on the top show the absolute value of the flux, while the plots in the bottom the normalized values. The following statements can be made:

- the absolute value of the flux is lower for the lower inclination angles 0° and 25°;
- the flux is reduced at the end of the pulse in all the cases;
- at the end of the plasma phase the normalized flux profile has changed in the case of 0° and 25°, while it is still stable in the other cases.

These results can be explained by taking into account that different inclinations of the nozzle imply the built up of the initial Cs reservoirs at different positions, in particular the higher the inclination angle, the more centered the Cs reservoirs. This is shown in the top part of figure 5, where the Cs coverage on the side wall after one vacuum phase is plotted for the four inclination angles. The maximum Cs coverage in a vacuum phase with an evaporation rate of 10 mg/h is around 4 monolayers (1 monolayer of Cs onto molybdenum is $\sim 4.5{\cdot}10^{14}$ atoms cm^{-2}).

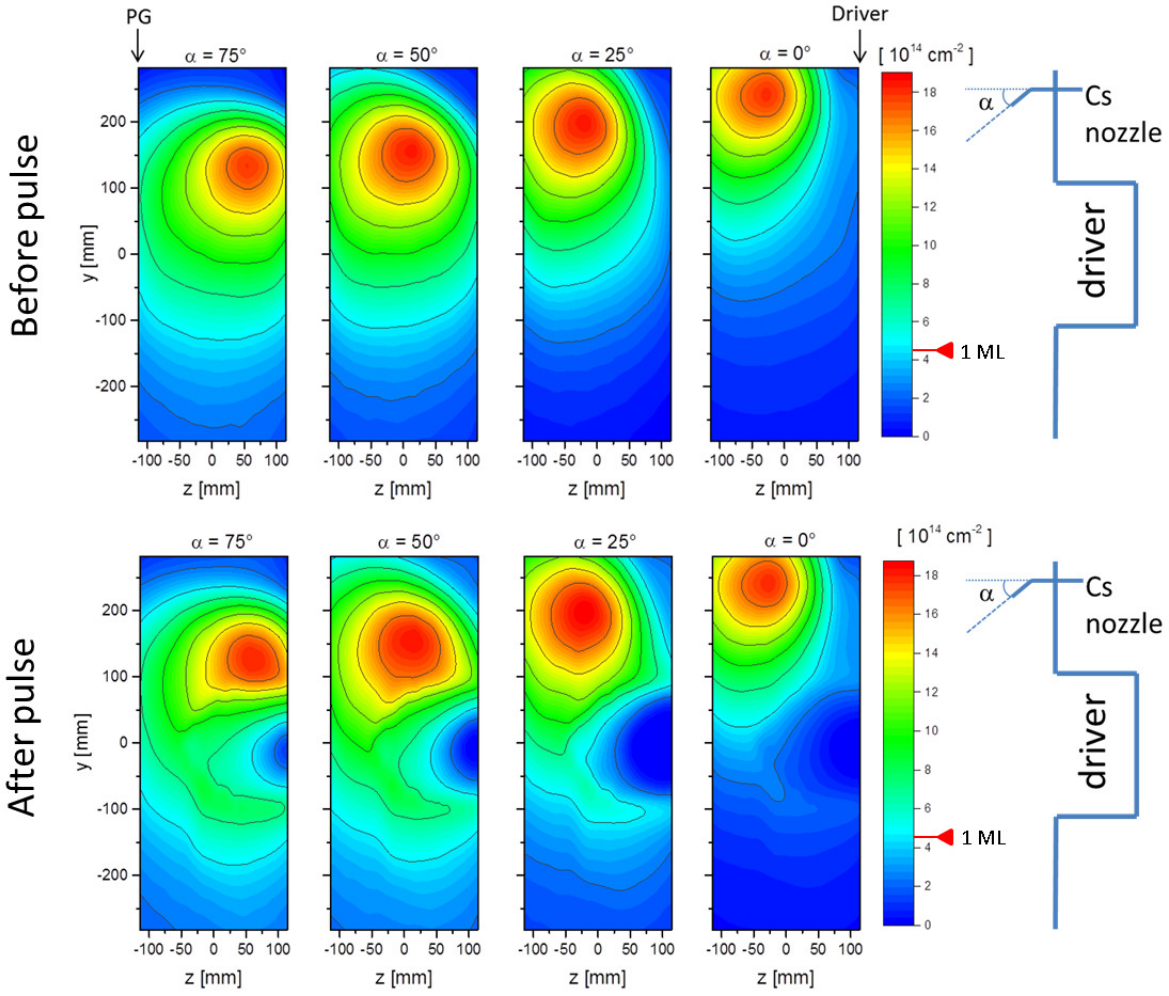

Figure 5: Cs coverage on the side wall of the IPP prototype source for different evaporation angles after 240 s vacuum phase (top) and after the following 8 s plasma pulse (bottom). The red arrow indicates the coverage correspondent to 1 monolayer (ML) of Cs onto Mo, i.e. $4.5{\cdot}10^{-14}\,\mathrm{cm}^{-2}$. Nozzle length 2.5 cm, $T_{wall} = 40\,^{\circ}\mathrm{C}$, $T_{PG} = 150\,^{\circ}\mathrm{C}$, Cs evap. rate 10 mg/h.

In all the cases a reduction of the Cs reservoirs on the surface is observed, which explains the reduction of the fluxes during the pulse. The rate of Cs erosion during the plasma pulse depends on the plasma density and it is higher close to the driver exit, where plasma density is also higher. If the amount of Cs in this area is enough to avoid the complete depletion of the reservoir during the plasma phase, no variation of the flux profile is observed onto the plasma grid (as in the case of 75° and 50°), while if the Cs coverage in this area is lower (as for 25° and 0°) the reservoirs will strongly reduce during the plasma pulse, thus influencing the stability of Cs flux onto the PG.

The bottom part of figure 5 shows the Cs coverage onto the lateral wall immediately after the pulse: the strong depletion of the reservoirs in the lower angle cases is evident. Hence, when designing the nozzle, it is important to take into account the relation

between the position of Cs reservoirs and the regions where plasma erosion is stronger, in order to achieve a better and more stable redistribution of the Cs from the wall reservoirs.

Another possible location for the Cs oven nozzle in the prototype source was also investigated, by considering another available port on the side of the expansion region, close to the plasma grid. In order to investigate the differences with respect to the previous case, i.e. with the oven positioned on the top of the back-plate, the source operation was simulated by positioning the Cs oven on the top of the diagnostic flange (sketch in figure 6b) and by changing the orientation angle between $-20°$ (evaporation towards the PG) and $+20°$ (evaporation towards the back-plate).

In figure 6a the average flux onto the plasma grid during a pulse is plotted as function of time: the dashed line represents the reference case with the oven in the back-plate. The plot shows that higher Cs fluxes are achieved with the oven in the diagnostic flange, w.r.t. the oven in the back-plate and in particular fluxes are higher by orienting the nozzle towards the back-plate. It can also be noticed that the time at which the flux reaches its maximum depends on the orientation: with the nozzle towards the PG the peak of Cs flux is reached earlier. These results suggest that a better stability and higher amount of Cs during the plasma phase can be achieved by evaporating Cs towards the back-plate, because in such a way the reservoirs will be located closer to the position where plasma erosion is more significant.

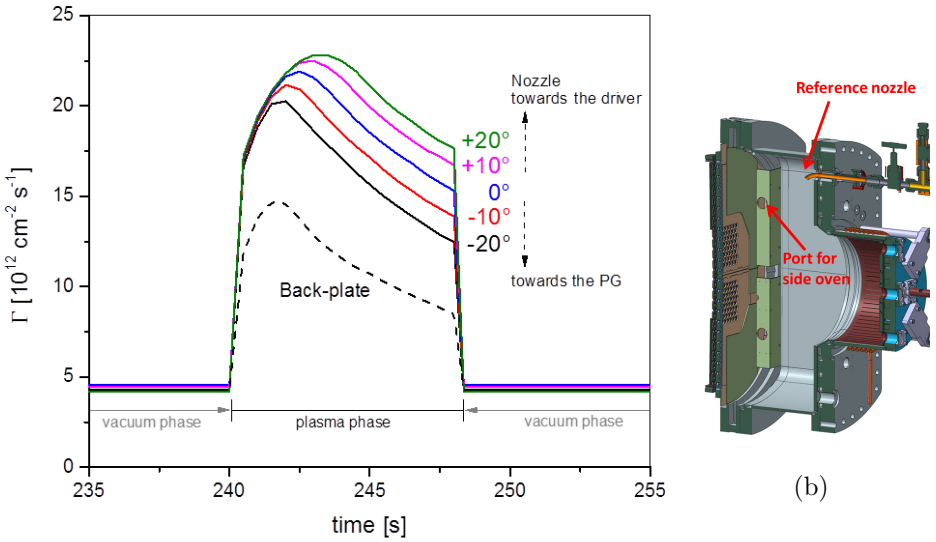

Figure 6: (a) Average Cs flux Γ onto the plasma grid for different nozzle orientation in the side wall (diagnostic flange) of BATMAN. Plasma pulse between $t = 240\,s$ and $t = 248\,s$; (b) Schematic showing the position of the port considered for the side oven.

6. Repetition of consecutive pulses

The results formerly presented have been calculated only for one single pulse after one vacuum phase, starting with no Cs deposited on the surfaces. The conditioning of the source during the experiments, i.e. lowering the PG work function and the achievement of good performances, is a process that need several cycles of vacuum phase and plasma pulse. It is an experimental evidence that the oven evaporation rate cannot be indefinitely increased in order to create the desired Cs reservoirs in a single vacuum phase, without affecting negatively the performances: if the evaporation rate is too high, an excessive amount of Cs in the driver can reduce the RF efficiency [21] and eventually increase the probability of breakdowns in the grid system [22]. Therefore, an accumulation of Cs only on the source walls but not on the driver is necessary, and this is achievable by repeating the cycle and exploiting plasma redistribution during the pulse.

The experimental conditioning process can be observed in figure 7 (a), which shows the experimental values of the extracted negative ion current and the intensity of neutral Cs emission line at 852 nm detected by a photodiode along a vertical line of sight close to the PG. The values are plotted versus the progressive pulse number during the conditioning phase. The Cs evaporation was started at pulse 102612: before the evaporation the Cs emissivity is constant at an offset value due to the molecular hydrogen background emission in the same wavelength [23]. The Cs oven temperature was increased in four steps as indicated in the figure. During the conditioning all source

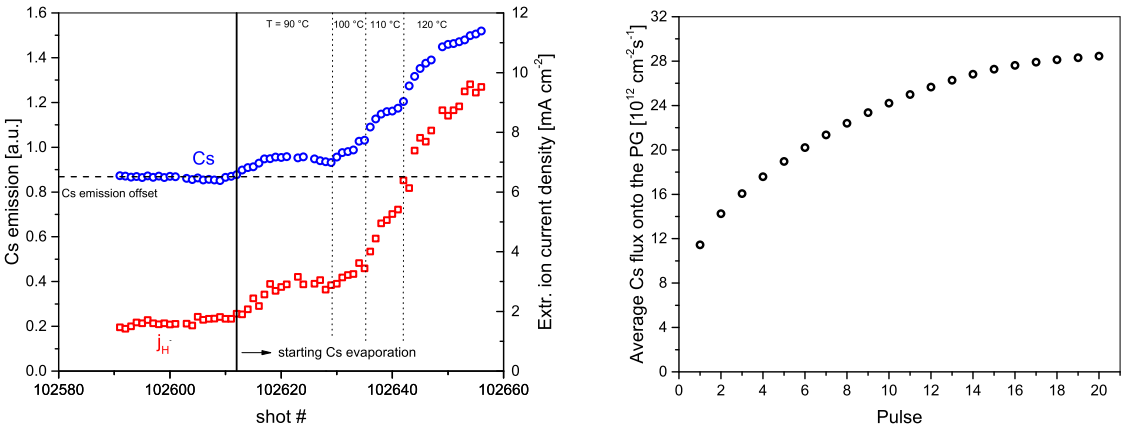

(a) (b)

Figure 7: (a) Experimental value of Cs emission at 852 nm measured by a photodiode (circles) and of the extracted negative ion current (squares) during the conditioning process at pressure 0.3 Pa and RF power 60 kW. (b) Average Cs flux onto the plasma grid during the plasma phase for consecutive pulses. Pulse length 8 s and vacuum phase time between the pulses of 240 s.

parameters were kept constant, i.e. RF power of 60 kW and pressure of 0.3 Pa. Once Cs is evaporated, the signal increases pulse by pulse and the extracted current follows the same trend.

In particular, inside every region with constant Cs oven temperature, the Cs emission increases at first and afterwards reaches a saturation value. This is a typical behaviour of the conditioning process, in which the increase of the available Cs in the source wall can provide more and more flux onto the plasma grid during the plasma phase, thus increasing the source performance.

In order to investigate this effect with `CsFlow3D` and compare the results with the experimental data, further simulations have been performed by repeating 20 times the standard pulse, starting with a clean source (no Cs deposited on the walls). Figure 7 (b) shows the total Cs flux onto the plasma grid, averaged on the grid area and on pulse time, for consecutive pulses, i.e. plasma pulses of 8 s with a vacuum phase time of 240 s between pulses with a constant evaporation rate of 10 mg/h as assumed in the previous simulations. The Cs flux onto the plasma grid increases pulse after pulse: in every vacuum phase the amount of Cs deposited in the inner surfaces of the source increases and therefore more Cs is available for the redistribution by the plasma during the following pulse. The saturation of the Cs flux onto the PG is reached after around 20 pulses. This evolution of Cs dynamics in time during the conditioning phase is similar to the experimental observations (considering the experimental regions with constant Cs evaporation rate).

In the next step the results of the calculations will be extensively compared with the experimental data from the prototype source in different operative scenarios in order to benchmark the code, in particular considering the effect of the plasma parameters distribution in the source. The results shown so far are relative to the prototype source at the BATMAN test facility, which was designed to investigate short pulses. The code can then be used to investigate the evolution of Cs dynamics also for longer pulses up to one hour in larger sources and be benchmarked against the data from the ELISE test facility, which is designed for long pulse operation. After the benchmarking, the code will be used to make predictive simulation of the full size ITER NBI source.

7. Application of CsFlow3D to the case of a race-track driver

The prototype source used at BATMAN has been used to test an alternative driver concept: the cylindrical driver has been replaced with a big race-track driver shape source [24]. This driver shape is already in use in positive RF ion sources such as the ones mounted on the ASDEX Upgrade machine [25]. Two constraints have to be taken into account in order to optimize the position and orientation of the Cs oven nozzle in negative ion sources: the amount of Cs which is deposited inside the driver during the vacuum phase and the amount of Cs which is lost throughout the plasma grid apertures and enters the extraction system. As mentioned in the previous section, it is an experimental observation that a high increase in the amount of Cs inside the driver

can lead to a reduction in the RF efficiency [21]. The presence of Cs into the extraction system can instead be harmful for the voltage holding, because of increased break-down probability [22].

Figure 8a shows a section of the prototype source with the race-track driver installed in comparison with the cylindrical driver (figure 8b). With respect to the cylindrical driver, there is no more the possibility of positioning the Cs oven nozzle in the back-plate of the expansion chamber. The only available ports for Cs evaporation are in the back-plate of the driver or on the diagnostic flange, on the side close to the plasma grid.

The race-track geometry was implemented in the code and simulations were performed by positioning the Cs oven either in the back-plate of the driver, using the different available ports with and without bending of the nozzle (i.e. cases A, B_0, B_{45} and C in figure 8a), and in the diagnostic flange close to the plasma grid (case S). The different cases are summarized in table 1. Two reference cases are taken into account for matter of comparison: the simulation of the prototype source with the cylindrical driver (figure 8b) and the oven on the top of the back-plate evaporating towards the plasma grid, and the simulation of ELISE (figure 8c), in which the nozzles are located in the side of the expansion chamber, oriented towards the back-plate. Since the evaporation towards the driver is the standard configuration used experimentally at the ELISE test facility, the results for this reference case can indicate the maximum level of Cs in the driver at which the source operation are possible without problems.

A typical vacuum phase of 200 s was simulated for the race-track driver in all the presented configurations. The output of the calculations are the total amount of accumulated Cs onto the driver surfaces (surface temperature set to 35°) and the average Cs loss flux, i.e. the number of Cs atoms which are lost through the aperture system per unit area and unit time. In order to compare the data among the three different sources, the Cs coverage on the driver surfaces was normalized to the total driver volume, since the key factor that can affect the RF coupling efficiency is the Cs density inside the driver.

Figure 9a shows the Cs coverage as a function of the nozzle angle for the oven positioned on the back-plate and on the diagnostic flange. The resulting Cs accumulation is much higher with the nozzle on the back-plate with respect to the diagnostic flange and to the reference cases. In the best cases A_{10} and B_0 the Cs in the driver is between 25% and 30% more than the amount for the ELISE reference case.

Case	Position	Nozzle. angle
A	Backplate	$\alpha = 0, 10, 20, 30, 40°$
B_0,B_{45}	Backplate	$\alpha = 0, 45°$
C	Backplate	$\alpha = 0, 10, 20, 30, 40°$
S	Diagnostic flange	$\beta = -10, 0, 10, 20, 30°$

Table 1: Simulated nozzle configurations for the BATMAN racetrack driver as indicated in figure 8a.

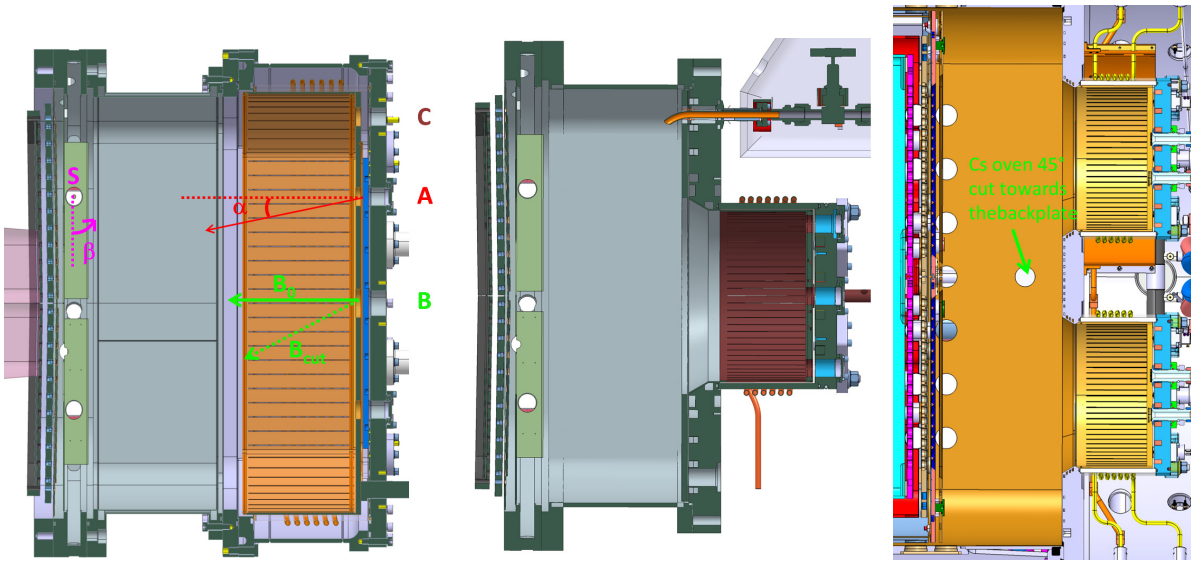

(a) (b) (c)

Figure 8: (a) source at the BATMAN test facility with racetrack driver. The different available ports for the Cs oven nozzle are indicated (A, B, C in the back-plate and S in the diagnostic flange); (b) Prototype source with cylindrical driver, oven nozzle on the back-plate, evaporation towards the grid; (c) source at ELISE, oven nozzles in the side wall, evaporation towards the back-plate.

In figure 9b the average Cs loss flux is plotted: all the position in the back-plate lead to a loss flux which is lower than the BATMAN reference case, while the position in the diagnostic flange leads to higher loss fluxes. Taking into account that these are averaged fluxes, the local loss flux towards the extraction system can be significantly higher than the reference, thus representing a problem for the high voltage holding.

The best compromise is therefore represented by the configuration B_0, i.e. the horizontal nozzle positioned in the center of the driver back-plate: the amount of Cs deposited on the driver walls is around 25% higher than the ELISE reference case, but it is possible to avoid the high Cs loss flux into the extraction region. In addition in this configuration any possible asymmetry of caesium redistribution due to the asymmetry of oven position is avoided, thus ensuring a more homogeneous caesiation of the PG.

This oven nozzle configuration has been implemented in the race-track driver and experiments have been performed. No repeated or severe break-downs in the extraction system due to Cs were observed during the operation and the evaporation of Cs from the back-plate of the driver did not represent a problem for the ignition of the plasma and for the achieving of good performances. The racetrack driver with the presented Cs nozzle configuration have in fact shown similar performances to the cylindrical driver [26].

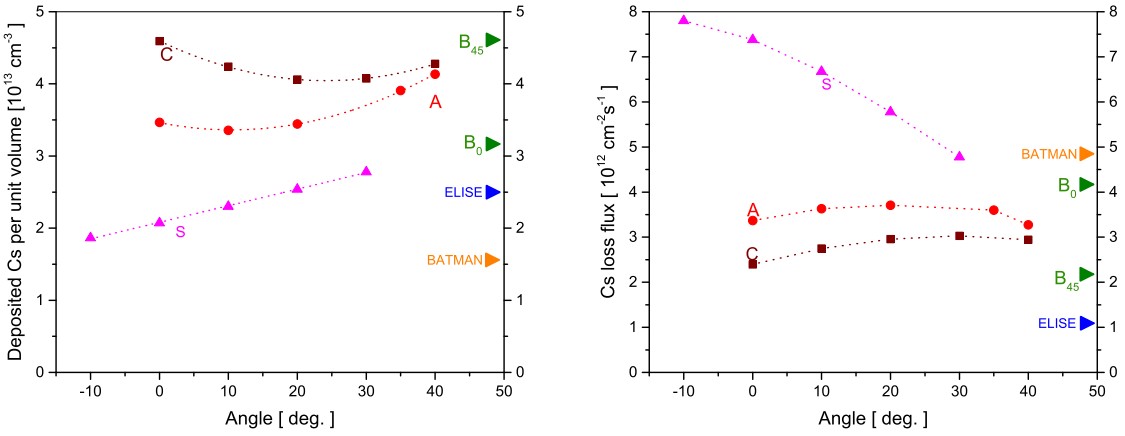

(a) (b)

Figure 9: Deposited Cs in the driver surfaces per unit volume (a) and Cs loss flux through the PG apertures (b) after a 200 s vacuum phase for the different nozzle configurations of the racetrack driver. The results for the two reference cases are reported as well, i.e. the cylindrical source in BATMAN (figure 8b) with the oven in the top back-plate and in ELISE (figure 8c), with the oven in the side of the expansion chamber.

8. Summary

In this work the Cs flow for two different nozzle geometries used in the negative ion sources at BATMAN and ELISE test facilities have been simulated: the calculated emission pattern has been used as input for the code. Furthermore the effect of the position and orientation of the Cs nozzle was investigated and the `CsFlow3D` code was applied to the race-track driver source in order to identify the best position and orientation of the Cs oven nozzle.

Results have shown that the flux of Cs onto the plasma grid during the plasma phase is mostly due to the erosion and redistribution of the Cs which is deposited on the source walls during the vacuum phase. In particular the position and orientation of the Cs nozzle have an effect on the amount and on the stability of Cs fluxes during the plasma phase, since a different evaporation configuration determines a different position of the Cs reservoirs on the walls. When the oven nozzle is positioned and oriented so that the Cs reservoirs build up in the region where the plasma erosion is larger (i.e. region where plasma density is higher), a better Cs redistribution occurs. This is a general rule that should be taken into account while designing the Cs oven nozzle configuration.

The conditioning process was also investigated: the code has shown that by repeating several time the cycle of plasma pulse and vacuum phase, the flux of Cs onto the PG increases pulse by pulse up to a stable level. This proves that the history of Cs redistribution due to the plasma plays a role in Cs dynamics and in the formation of the Cs reservoirs on the wall. This behaviour is comparable with what has been

observed in the experiment.

Further investigations are needed in order to study the evolution of Cs dynamics during long pulses, which are the target of the ITER-NBI sources. The results of the simulations will be then benchmarked and compared with the experimental data from the test facilities BATMAN and ELISE, in order to have a reliable, predictive and versatile simulation tool, which can be easily applied to sources of any geometry and configuration. This is a basic step towards more efficient and reliable Cs management as well as a reduction of Cs consumption in negative ion sources for fusion, two targets that are of fundamental importance also for the future development of industrial demonstrational power plants such as DEMO.

Acknowledgments

This work has been carried out within the framework of the EUROfusion Consortium and has received funding from the Euratom research training programme 2014-2018 under grant agreement 633053. The views and opinions expressed herein do not necessarily reflect those of the European Commission.

References

[1] R. Hemsworth et al., *Nucl. Fusion*, **49**, 045006 (2009)
[2] K.H. Berkner, R. V. Pyle and J. W. Stearns, *Nucl. Fus.* **15**, 249 (1975)
[3] A. Krylov and R.Hemsworth *Fusion Eng. Des.*, **81**, 223948 (2006)
[4] Y. I. Belchenko, G. I. Dimov, and V. G. Dudnikov, *Nucl. Fusion* **14**, 113 (1974)
[5] B.S. Lee and M. Seidl, *Appl. Phys. Letters* **61**, 2857 (1992)
[6] R. Gutser, C. Wimmer, and U. Fantz, *Rev. Sci. Instrum.* **82**, 023506 (2011)
[7] E. Speth, H. Falter, P. Franzen, U. Fantz et al, *Nucl. Fus.* **46**, 220 (2006)
[8] U. Fantz et al., *Rev. Sci. Inst.* **87**, 02B307 (2016).
[9] P. Franzen et al., *Plasma Phys. Control. Fusion*, **53**, 115006 (2011)
[10] M. Fröschle et al., *Fus. Eng. Des.*, **84**, 788 (2009)
[11] U. Fantz, R. Friedl, M. Fröschle, *Rev. Sci. Inst.* **83**, 123305 (2012)
[12] R. Gutser, C. Wimmer, and U. Fantz, *Rev. Sci. Inst.* **82**, 023506 (2011)
[13] R. Gutser, U. Fantz and D. Wünderlich, *Rev. Sci. Inst.* **81**, 02A706 (2010)
[14] U. Fantz, R. Gutser and C. Wimmer, *Rev. Sci. Inst.* **81**, 02B102,(2010)
[15] S. Ma, R.D. Sydora, J.M. Dawson, *Comput. Phys. Commun.* **77**, 190 (1993)
[16] M. Lukomski et al., *Phys. Rev. A* **74**, 032708 (2006)
[17] D. Lide, *CRC Hanbook of Physics and Chemistry, 88th edition*, CRC (2007)
[18] R. Gutser, D. Wünderlich, U. Fantz, *Plasma Phys. Control. Fusion* **53**, 105014 (2011)
[19] G. A. Bird, *Molecular gas dynamics and the direct simulation of gas flows*, Clarendon Press, Oxford (1994).
[20] G. A. Bird, *DSMC resource from Graeme Bird*, http://gab.com.au/downloads.html (updated 2013)
[21] B. Heinemann et al., *New J. Phys.* **19**, 015001 (2017)
[22] Yu. Belchenko et. al., *Rev. Sci. Instrum.* **87**, 02B120 (2016)
[23] G.H. Dieke, *J. Mol. Spectroscopy* **2**, 494 (1958)
[24] B. Heinemann et al., *AIP Conf. Proc.* **1655**, 060003 (2015)
[25] Speth E. and NBI Team, *Plasma Sci. Technol.* **6**, 2135 (2004)
[26] C. Wimmer, U. Fantz, E. Aza et al., *AIP Conf. Proc.* **1869**, 030021 (2017)